

DOI: 10.15825/1995-1191-2023-4-160-173

SAFETY ASSESSMENT OF THE FEMTOSECOND LASER IN CORNEAL LIMBAL GRAFT EXCISION

O.N. Nefedova¹, B.E. Malyugin^{1, 2}, S.A. Borzenok^{1, 2}, M.Yu. Gerasimov¹, D.S. Ostrovsky¹, A.V. Shatskikh¹

¹ Fyodorov Eye Microsurgery Federal State Institution, Moscow, Russian Federation

² Moscow State University of Medicine and Dentistry, Moscow, Russian Federation

Objective: to study *in vitro* survival and preservation of the proliferative activity of limbal stem cells (LSCs) in femtosecond laser-cut limbal tissue fragments. **Materials and methods.** Limbal fragments were formed from donor cadaver eyes (n = 8) in the upper and lower limbus containing the highest number of limbal stem cells, using a Z8 femtosecond laser (FSL) (Ziemer, Switzerland). The limbal fragments were fragmented into 4 mini-grafts using different energy levels (100, 110, 120%). Mini-grafts from symmetrical sections of the cadaver eyes, which were manually isolated using a microsurgical blade, served as controls. The mini-grafts were cultured for two weeks in culture media intended for limbal epithelial stem cells (LESCs) (EpiLife (0.06 mM Ca⁺⁺) and for multipotent mesenchymal stem cells (MMSCs) (DMEM/F12), with the addition of specific growth factors to selectively stimulate LESCs or MMSCs, respectively. The phenotype of the obtained cultured cells in the “laser” and “knife” groups was determined by flow cytometry using a set of markers (CD166, CD105, CD90, CD29, CD34) for the membrane proteins of LESCs and MMSCs. The ability of cultured cells to adhesion and proliferation in the “laser” and “knife” groups was determined by seeding the third passage of the resulting cultures on Bowman’s membrane of acellular corneas. **Results.** Primary cell culture was obtained from mini-grafts of all donors in both groups. Cell morphology was consistent with the phenotype of corneal epithelial cells (cobblestone pattern). When cultured in the EpiLife medium (0.06 mM Ca⁺⁺), we determined the presence of LSCs proliferation from 38.6% of mini-grafts; in the DMEM/F12 medium (1 : 1) the presence was determined from 31.8%. Two weeks later, cell yield from mini-grafts in the “laser” and “knife” groups was 77.2% and 63.6%, respectively. Cell growth by the end of week 2 of culturing of mini-grafts obtained by FSL at 120, 110 and 100% energies was 87.5, 71.4 and 71.4%, respectively. It was found that the resulting cell cultures in the “laser” and “knife” groups and in the “120%”, “110%” and “100%” subgroups were not different phenotypically. Cytofluorimetric analysis showed that cell cultures in the groups had a mixed pattern of marker expression of both LESCs (CD29+) and MMSCs (CD90+, CD105+). Seeding of the third passage of cell culture in the test groups in all cases demonstrated adhesion and formation of a cell monolayer on the Bowman’s membrane of model corneas. **Conclusion.** The use of FSL for cutting out limbal grafts seems to be effective and safe in comparison with the traditional mechanical (knife) technique. Cell cultures obtained from FSL-cut mini-grafts were able to grow and migrate for at least 21 days.

Keywords: limbal stem cells, glueless simple limbal epithelial transplantation, limbal stem cell deficiency, femtosecond laser.

INTRODUCTION

Corneal transparency depends on several factors, among which the epithelial layer is one of the most important. The layer functions as an effective barrier separating the cornea both from the external environment and from the spread of conjunctival epithelium on it. The corneal epithelium is continuously renewed by LESC. The vector of cell movement is directed from Bowman’s membrane to the corneal surface and from its periphery to the center [1]. LESC cells reside in the limbus, which is a complex micro-anatomical structure [2]. The proliferation, migration, and differentiation of LESCs are dependent upon their specialized microenvironment known as the limbal niche. In addition to limbal epithelial

progenitor cells, the limbal niche contains MMSCs, melanocytes, immune cells, vascular and nerve cells, extracellular matrix and signaling molecules (growth factors and cytokines) [3–8].

Various pathologies affecting any component of the limbal niche can lead to limbal stem cell (LSC) dysfunction and, consequently, to limbal stem cell deficiency (LSCD) [7, 9, 10]. The causes of this condition may be primary, caused by genetic defects (congenital aniridia, Peters anomaly), systemic autoimmune diseases (Stevens–Johnson syndrome, ocular cicatricial pemphigoid) and acquired – due to trauma or chronic inflammatory processes (chemical and thermal burns, chronic long-term keratitis and keratoconjunctivitis, neurotrophic and

bullous keratopathies, toxic-allergic reactions, ocular surface tumors, etc.) [11].

LSCD is classified into complete and incomplete depending on the amount of damage to the limbal zone. Depending on the involvement of each eye in this pathological process, bilateral or unilateral LSCD is distinguished [12].

The most promising and safe treatment option for unilateral LSCD (complete and incomplete), which has been widely used in the world, is simple limbal epithelial transplantation (SLET), described in 2012 by V. Sangwan et al. [12, 13]. For this technology, it is necessary to isolate a 2×2 mm section of the upper corneal limbus from a healthy eye and dividing it with a microsurgical blade into several (8–12) fragments, gluing them with fibrin glue to the amniotic membrane overlaid on top of the previously prepared corneal stroma of the damaged eye [13]. Since a relatively small volume of limbal tissue of the donor eye is taken, the risk of iatrogenic LSCD in the healthy eye is minimized. The efficiency of this operation is 80% or more in adult patients and 71.2% in children [14].

The glueless simple limbal epithelial transplantation technique (G-SLET) was proposed as an alternative to the SLET technique and does not involve the use of fibrin glue [15]. After removal of the fibrovascular pannus from the surface of the damaged eye, the resulting limbal flaps are fixed by placing them in tunnels formed on the periphery of the corneal stroma. Thus, a peculiar “depot” of limbal stem cells located in the peripheral part of the cornea is formed [15].

It should be noted that in both SLET and G-SLET techniques, all manipulations on cutting and fragmentation of the limbal graft are performed manually, mechanically using microsurgical instruments (a delaminator, a disposable non-dosed metal blade or a dosed diamond knife, microtweezers) [12, 13]. It is difficult to achieve uniformity in the limbal flap throughout its length; the quality of the obtained grafts depends on the surgeon's experience and is difficult to standardize. In the absence of methods to control the incision depth, excessively shallow or uneven dissection may significantly limit the production of sufficient LSC volume for successful reconstruction of the corneal epithelium. The limbal graft fragmentation stage and subsequent graft manipulation, in particular compression with forceps, can lead to damage and even death of a part of the LSC. Transferring an insufficient amount of LSC can significantly reduce the effectiveness of the operation.

The introduction into practice of FSL technologies for tissue dissection, ensuring the formation of uniform and dosed cuts, as well as the units having in their interface high-precision visualization systems based on optical coherence tomography (OCT), is an extremely relevant and promising direction in ophthalmic surgery. From our point of view, the use of FSL has a real potential to obtain

a full-fledged limbal graft with full capture of the LSC niche with its microenvironment and minimal damage compared to the mechanical method. In the available literature, we did not find information about the use of FSL for SLET technology, as well as articles studying the effect of laser energy on LSC survival after corneal limbal laser extraction, which was the basis for this study.

The **objective of the study** was to investigate in an in vitro experiment the survival and preservation of the proliferative activity of LSCs in femtosecond laser-cut limbal tissue fragments.

MATERIAL AND METHODS

Obtaining limbal grafts containing LSCs

Experimental studies on tissues isolated from cadaveric human donor eyes were performed in accordance with the legislative and regulatory documents of the Russian Federation. Limbal eyeball transplants ($n = 8$) from deceased male donors ($n = 4$) aged 55.3 years (32–71 years), provided by the Eye Tissue Bank (ETB) from Fyodorov Eye Microsurgery after infectious screening and decontamination with 10% povidone-iodine solution (EGIS, Hungary) according to the algorithm for preparation of donor corneal cadaveric material in the ETB [16]. Cleaning from the corneal epithelium and removal of residual tissues at the limbus were not performed. Donor corneas that were unsuitable for transplantation in the clinic due to low endothelial density or stromal defects were used for the experiment. The time from the moment of ascertaining biological death to the extraction of tissue fragments was 18.8 ± 0.5 hours.

Limbal grafts were obtained in the operating room in compliance with all asepsis and antisepsis rules. The eyeballs were fixed in a sterile mechanical holder. The upper portion of the corneal limbus was determined by the remnants of the upper rectus muscle, and markings were made. Limbal flaps were excised using FSL in the meridian from 12 to 2 and from 4 to 6 of the conditional dial (experiment) (Fig. 1) at energy levels equal to 100%, 110%, and 120% (high-frequency low-energy

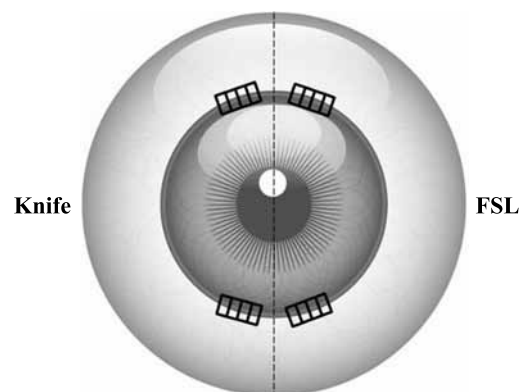


Fig. 1. Schematic of limbal mini-graft excision from donor cornea

FSL (nJ), horizontal cutting depth 200 μm), after which limbal flaps were excised in the meridian from 10 am to 12 noon and from 6 to 8 p.m with a manually dosed diamond knife and a dissecting knife (control) (Fig. 1). A 1.0 mm intact limbal section (lintel) was left between two limbal graft samples, different by the method via which they were obtained.

The technique for forming limbal fragments was as follows: a limbal graft 2.0 mm long, 1.5 mm wide was fragmented into 4 equal parts (mini grafts) (Fig. 1). In the upper and lower limbus of each eye on the left side, the limbal graft was cut out mechanically using microsurgical instruments (control). For this purpose, based on the marking in the upper and lower limbus, we made cuts with a diamond knife at a 200 μm depth, which, according to our estimations, is optimal for fully capturing the limbal niche with its microenvironment. After contouring, using a dissecting knife, the limbal graft was separated from the underlying tissues. Next, it was carefully transferred to a polymer substrate and divided into 4 equal parts (mini-grafts) using a steel microsurgical disposable blade. In the right part of the limbus (both above and below), formation of a limbal graft and its single-step division into 4 parts was carried out using FSL. For this purpose, after appplanation of the laser handle to the cadaveric eye, the cutting trajectories were positioned, and the estimation of the horizontal cutting depth was controlled by the built-in OCT system. The laser operation time for the formation of one limbal graft with its fragmentation was 40 seconds. To evaluate the effect of different FSL energies on LSC growth, limbal grafts were cut out on different eyes at different energy levels (100%, 110%,

and 120%). The selected levels were determined based on our previous studies of different energy values on the fragments formed. A total of 128 mini-grafts were obtained during the experiment (Fig. 2).

The resulting mini-grafts were placed into pre-prepared sterile microcentrifuge tubes with 500 μL of corneal storage solution (RU FSR № 2010106650, Eye Microsurgery, Russia). Then the labeled tubes were placed in a container and transported to a laboratory at Center for Fundamental and Applied Biomedical Problems (CFA-BP) under the head office Fyodorov Eye Microsurgery.

Cultivation of corneal limbal mini-grafts

Experiments on mini-grafts cultivation were performed at the CFABP laboratory under sterile in vitro conditions. Cultivation was carried out under standard conditions: +37 °C, 100% humidity and 5% CO₂ concentration (incubator NU-5510 NuAire, USA). For this purpose, each obtained mini-graft was placed in a separate well of a 48-well plate (#30048, SPL Lifesciences, Korea) with epithelial part upwards, 40 μL of culture medium was added and transferred to a CO₂ incubator; after 2 hours another 100 μL of medium was added. After 24 hours, the standard volume of medium was used (500 μL per well). The medium was changed every 2–3 days.

Cultivation was carried out in two media until the 3rd passage. To stimulate LSCs growth, EpiLife medium with 0.06 mM Ca⁺⁺ (MEPICFPRF500, Gibco, USA) was used, with the addition of an antimycotic antibiotic (A5955, Sigma Aldrich, USA): 100 U/mL penicillin, 100 $\mu\text{g}/\text{mL}$ streptomycin and 0.25 $\mu\text{g}/\text{mL}$ amphotericin B, 5% fetal bovine serum (SH30109. 03, HyClone Laboratories, USA), 5 $\mu\text{g}/\text{mL}$ soluble human genetically engineered short-acting insulin (Humulin Regular, Eli Lilly and Company, USA), 5 $\mu\text{g}/\text{mL}$ hydrocortisone (Pharmak, Ukraine) and 10 ng/mL human recombinant epidermal growth factor (hEGF) (FR-08000, PanEco, Russia) [17, 18]. The other part of the samples was cultured in DMEM/F12-based limbal MMSCs medium with 1.05 mM Ca⁺⁺ (D6421, Sigma Aldrich, USA), supplemented with similar components [17, 18].

Once the cells reached 80–90% confluency, the culture was passaged using accutase enzyme (StemPro™ Accutase™ Cell Dissociation Reagent, A1110501, Gibco, USA). To do this, culture medium was removed from each well, 300 μL of enzyme was added and removed for debris clearance. Then 300 μL of accutase was re-added and placed in a CO₂ incubator at 37 °C for 10 minutes. The cell suspension was collected into a 15 mL centrifuge tube, precipitated for 5 minutes at 200 g at room temperature, and resuspended in 1 mL of culture medium. 10 μL of the suspension was used to count cells in a LUNA-II™ counter (Logos Biosystems, Korea).

Daily intravital observation of the mini-grafts and cell cultures was performed using an inverted phase-contrast microscope Olympus IX81 (Olympus, Japan). Images

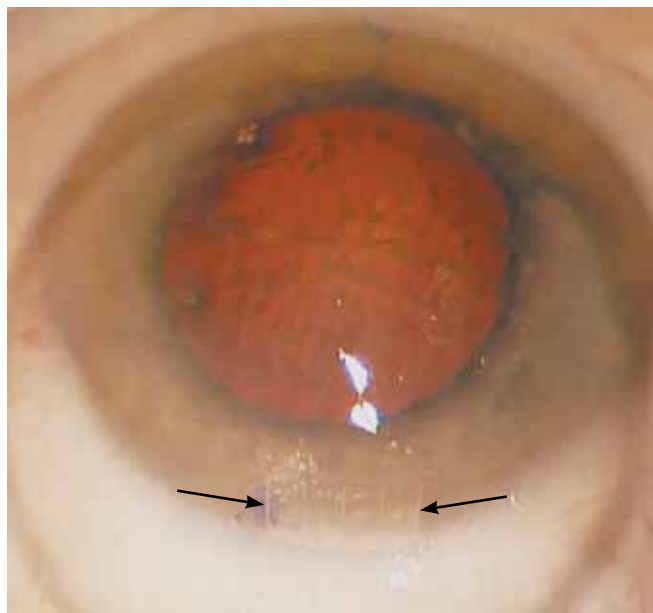


Fig. 2. Photo of the donor eye after cutting out limbal mini-grafts with a femtosecond laser. Four mini-grafts are visible, the lateral borders of the laser incisions are indicated by arrows

were prepared in the internal program environment of the microscope (CellSence).

Statistical analysis

Categorical data were used to statistically analyze the results obtained. The categorical data included three numerical values (0, no adhesion and growth; 1, mini graft fixed; 2, mini graft fixed and there is cell yield). Statistical analysis included three tests:

The first test was to determine the effect of the media used (DMEM/F12 and EpiLife) on mini graft adhesion and cell yield using the “2×2 table” method with calculation of Fisher’s exact test with two-sided hypothesis testing.

The second test was to determine the confidence limits, which allows to calculate the distribution of the attribute data over the sample and to determine the true value of the given parameters in the whole sample with a 90% probability. The modified Wald method was used to determine the confidence limits.

The third test was to calculate the probability of a positive event (we consider a positive event to be the attachment of a piece, as well as the attachment and active exit of cells from it). The binomial test was used, namely the sign test, which suggests that the event and its absence are equally likely to have a 50% probability.

Immunophenotyping of cell culture from corneal limbal mini-grafts

To determine the immunophenotype, the third passage culture suspension of cells, cultured on a DMEM/F12 medium, was divided into tubes of five equal parts (260,000 cells per tube), and washed from the complete cell culture medium in 2 mL of buffer (CellWASH, BD, USA), twice for 5 minutes each. The resulting cell sediment was stained using a set of markers to membrane proteins CD105, CD90, CD166, CD29, CD34 (Biolegend, USA); the markers were conjugated with fluorochromes according to the manufacturer’s protocol. For this purpose, each tube was incubated at 25 °C in the dark for 15 minutes with antibodies (at the rate of 10 µL of antibody solution per 1 million cells). After incubation, the precipitate was resuspended in 1.0 mL of buffer and precipitated at 200 g for 5 min. The precipitate was then resuspended in 500 µL of buffer and analyzed on a CytoFLEX® flow cytometer (Beckman Coulter, USA). Immunoexpression curves were generated using the internal software of the device.

Study of the adaptation and adhesive properties of cell culture from corneal limbal mini-grafts

Donor human corneas that were unsuitable for transplantation were used for the experiment in the form of four corneoscleral discs.

Cornea preparation (cold cell elimination) was performed after completing all the donor corneal material preparation stages according to the previously described method [19]. Corneas were prepared in such a way that the entire epithelium was completely removed up to the Bowman’s membrane, and the limbus was cleared of the remaining conjunctival tissue. Then, the resulting corneal discs were individually placed in new sterile transparent vials containing corneal storage solution (RU FSR № 2010106650, Eye Microsurgery, Russia) and they were left at +4 °C for 45–62 days. The condition of the corneal discs was monitored by the color of the solution (red-orange and transparent if not contaminated). Before cell seeding, the corneoscleral discs were washed twice in phosphate buffered saline (PBS) for 2 hours at room temperature, after which the central corneal section was cut out using a 6.0-mm-diameter trephine blade (Barron, Katena Products, Inc, USA) and placed in the well of a 96-well plate (32496, SPL Lifesciences, South Korea) with the Bowman’s membrane to the outside and Descemet’s membrane to the surface of the bottom of the well.

To assess the ability of cultured LSCs to adhere to the Bowman’s membrane of the donor cornea, LSCs of the third passage were seeded onto prepared corneal discs located in the wells of the plate. Cell suspensions derived from mechanically excised mini-grafts (control) and using FSL (experiment) at different energy levels were used. LSC suspensions were seeded on the anterior surface of corneal discs at the rate of 140,000 cells per disc (1238.49 cells per 1 mm²). Cultivation was performed under standard conditions for 14 days using EpiLife medium (0.06 mM Ca⁺⁺) and LESC supplements as described above. The culture medium was changed every 2–3 days. Intravital observation was performed using an Olympus IX81 inverted phase-contrast microscope. Images were acquired in the internal software environment of the microscope (CellSence).

Histological examination of corneas

After day 14 of culturing, the corneal discs were prepared for subsequent histological analysis. They were removed from the wells and washed three times in PBS for 10 minutes. Each was then fixed in 10% neutral formalin solution (141328, AppliChem, Germany) for 24 hours and cut in half to make transverse sections. Next, the corneal disc halves were washed with running water and dehydrated in alcohols of ascending concentration. Then they were embedded in paraffin, and a series of 10 µm-thick histological sections were stained with hematoxylin and eosin according to the standard technique. The preparations were studied and photographed using an Olympus IX81 inverted phase-contrast microscope in a transmitted light mode at 40× and 100× magnifications.

The resulting photographs were analyzed in Fiji software (ImageJ 2.0.0-rc69/1.52) [20]. Statistical pro-

cessing was performed on a personal computer using statistical programs.

RESULTS

Obtaining primary LSC culture *in vitro*

On day 3 of cultivation, it was noted that primary attachment of mini-grafts was not achieved in all wells. It is known that for full LSC growth, dense adhesion to the surface of the culture well is necessary, and the lack of fixation of mini-grafts leads to formation of debris, death of differentiated cells, and, in some cases, lack of formation of a monolayer of the primary cell culture. Therefore, to prevent this phenomenon, a cohesive viscoelastic ProVisc (Alcon, USA) containing 1.0% sodium hyaluronate and having a neutral pH was used once, according to the guidelines in a number of previously published works [21, 22]. For this purpose, the culture medium was completely removed from the well and 2 drops of viscoelastic were applied to the mini-graft. Then 500 μ L of complete cell culture medium was added drop by drop and transferred to the incubator. For the first and subsequent examinations, slide plates were moved extremely carefully to the incubator, taking care to hold the incubator door when closing and opening to prevent shaking the mini grafts.

The first control examination after the beginning of cultivation was performed on day 7, further control examinations were performed every 3 days.

When examined on day 7 of cultivation, 31.25% of mini-grafts ($n = 40$) of the total number of wells were not fixed to the surface, they floated freely in the culture medium. At the end of culture on day 14, no growth was observed from the unfixed mini-grafts; large amounts of debris and dead undifferentiated cells were freely floating in the culture medium.

Primary cell culture was obtained in all samples that were adhered to the culture surface (68.75% of mini-grafts, $n = 88$). Morphologically, the primary culture cells followed the typical cobblestone pattern in all wells in both groups. Specifically, the cells formed a monolayer from the mini-graft, had a large nucleus and were tightly adhered to each other. At the same time, there was some variation in cell size and shape, more in line with the morphology of MMSCs, more pronounced for samples cultured in DMEM/F12 medium. Throughout the entire period of cultivation, the epithelial cell-specific morphology and the relative uniformity of their sizes were preserved in the primary culture.

In mini-grafts fixed to the surface of the wells and cultured in DMEM/F12, the first areas of cell growth were observed on day 5 from the start of cultivation. From the edge of the mini-graft, small cell clusters were formed, morphologically similar to LSCs, having a round shape and a large nucleus. In some samples, elongated cells with small nuclei (MMSCs) were observed

by day 7. As they grew, they spread along the surface of the socket further from the mini-graft, forming cavities. The closer the formed cavities were to the mini-graft, the more they were filled with LSCs. It was noted that in samples where MMSCs were found, the number of LSCs was much higher (Fig. 3).

When cultivated on an EpiLife-based complete cell culture medium, the first signs of growth were also noted on day 5. On day 7 of observation, both MMSCs and LSCs were observed in the primary culture (Fig. 4).

Overall, cell growth in EpiLife medium from the initial passage to completion of culture on day 14 was slower compared to mini grafts cultured in DMEM/F12 medium. However, at the final observation period on day 14, the number of wells with adherent mini-grafts and cell growth was 38.6% in the EpiLife medium, while it was 31.8% in the DMEM/F12 medium (Table 1). Cell culture on the EpiLife medium had characteristic differences: mostly small polygonal cells with a large nucleus were present, there were small areas with larger cells and a relatively smaller nucleus, which is typical for maturing cells.

LSC proliferation depending on the mini-graft isolation method

After 7 days from the start of cultivation, there was a higher number of proliferating cells from the mini-grafts obtained by the traditional method using microsurgical instruments compared to the growth of cells recorded in the wells with mini-grafts obtained by FSL excision, 45.4% and 31.8%, respectively. However, at follow-up examination on day 11, there was an advance in the growth rate in the FSL-obtained samples. By the last observation period on day 14, the number of wells with recorded cell growth from the FSL mini-grafts was noticeably higher, 77.2% in contrast to the control group, 63.6% (Table 2).

Table 1

Percentage number of wells with fixed growth of LSCs depending on culture medium

Observation period	DMEM	EPL
Day 7	20.4%	18.1%
Day 11	22.7%	20.4%
Day 14	31.8%	38.6%

Table 2

Percentage number of wells with fixed growth of LSCs depending on the method of obtaining mini-grafts

Observation period	FSL	Mechanical method
Day 7	31.8%	45.4%
Day 11	59.0%	54.7%
Day 14	77.2%	63.6%

LSC proliferation depending on FSL energy level

When analyzing cell proliferation, from mini-grafts obtained by dissection at different energy levels, differences in growth rate and number of wells with cell growth were found. The best proliferation rates at the observation period of 7 days were demonstrated by the samples of mini-grafts obtained using a 110% FSL energy level (42.8%), and the lowest growth rates were recorded at an FSL energy level of 120% (25%). The

growth pattern changed dramatically on day 11 of observation and the best growth rates were already demonstrated in the samples obtained with a 120% level of expended FSL energy (75%), the lowest growth rates in the samples with 100% level of FSL energy (42.8%). By the last observation period on day 14, in wells with mini-grafts obtained under 100%, 110% and 120% FSL energy levels, cell growth was 71.4%, 71.4%, and 87.5%, respectively (Table 3).

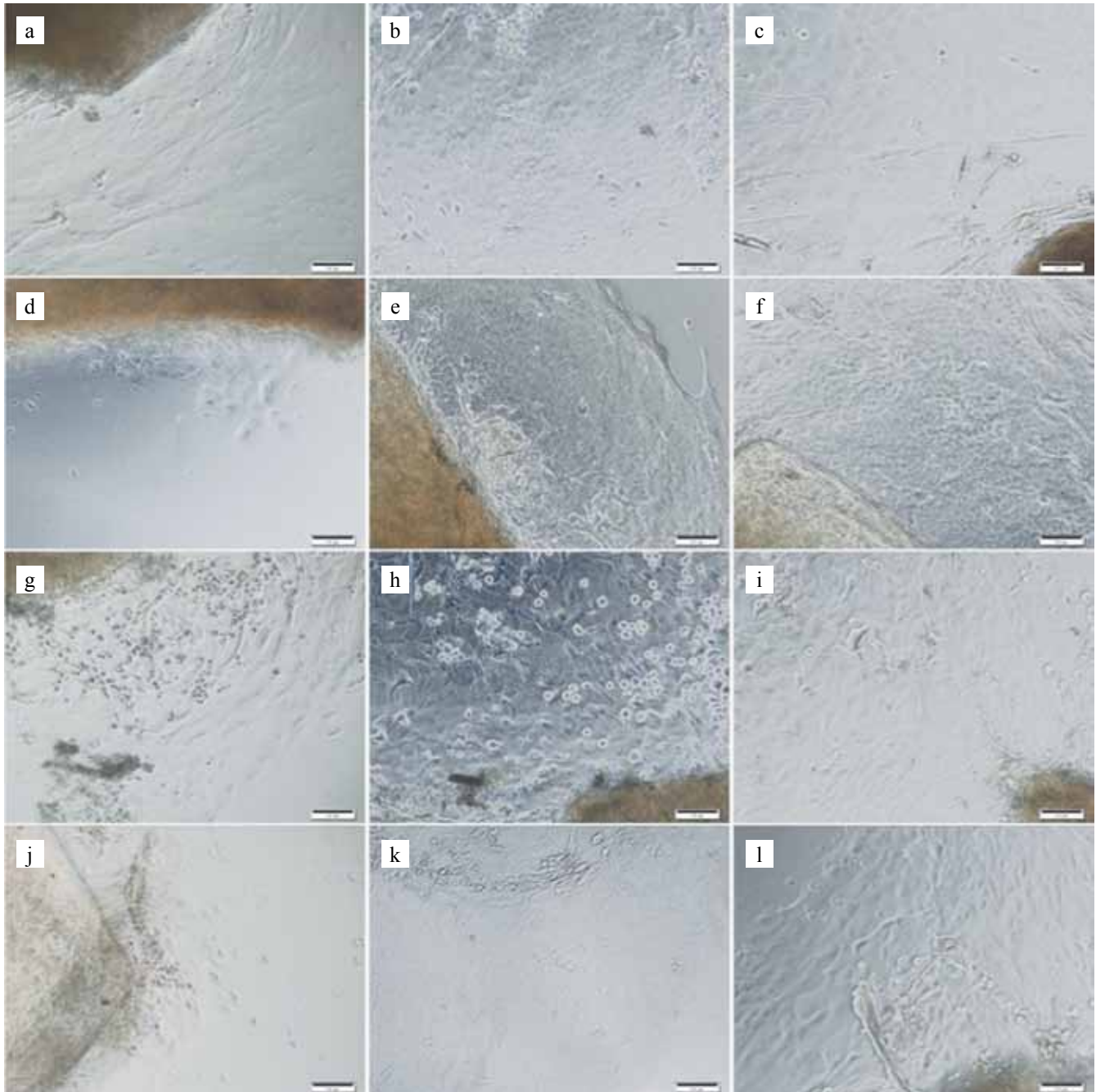


Fig. 3. Cell culture obtained from all types of mini-grafts on a DMEM/F12 medium. Different observation times (horizontally from left to right – days 7, 11 and 14 of culturing, respectively). (a, b, c), cell culture from mini graft obtained using 100% FSL energy level; (d, e, f), cell culture from a mini graft obtained using 110% FSL energy level; (j, h, i), cell culture from a mini-graft obtained using 120% FSL energy level; (j, k, l), cell culture from a mini graft obtained using microsurgical instruments. Light phase-contrast microscopy. Magnification 100×

Table 3 **Statistical analysis**

**Percentage number of wells
with fixed growth of LSCs depending
on the FSL energy level expended to excise
mini-grafts**

Observation period	100% energy	110% energy	120% energy
Day 7	28.5%	42.8%	25.0%
Day 11	42.8%	57.1%	75.0%
Day 14	71.4%	71.4%	87.5%

When determining the influence of the used media (DMEM/F12 and EpiLife) on mini-graft adhesion and cell yield by the “2×2 table” method with the calculation of Fisher’s exact test with the two-sided hypothesis testing, it was shown that the given compositions of the media do not statistically affect cell adhesion and cell yield in the knife and laser groups significantly ($p > 0.05$). However, it was shown that there is a statistically significant association of the signs between the “laser”

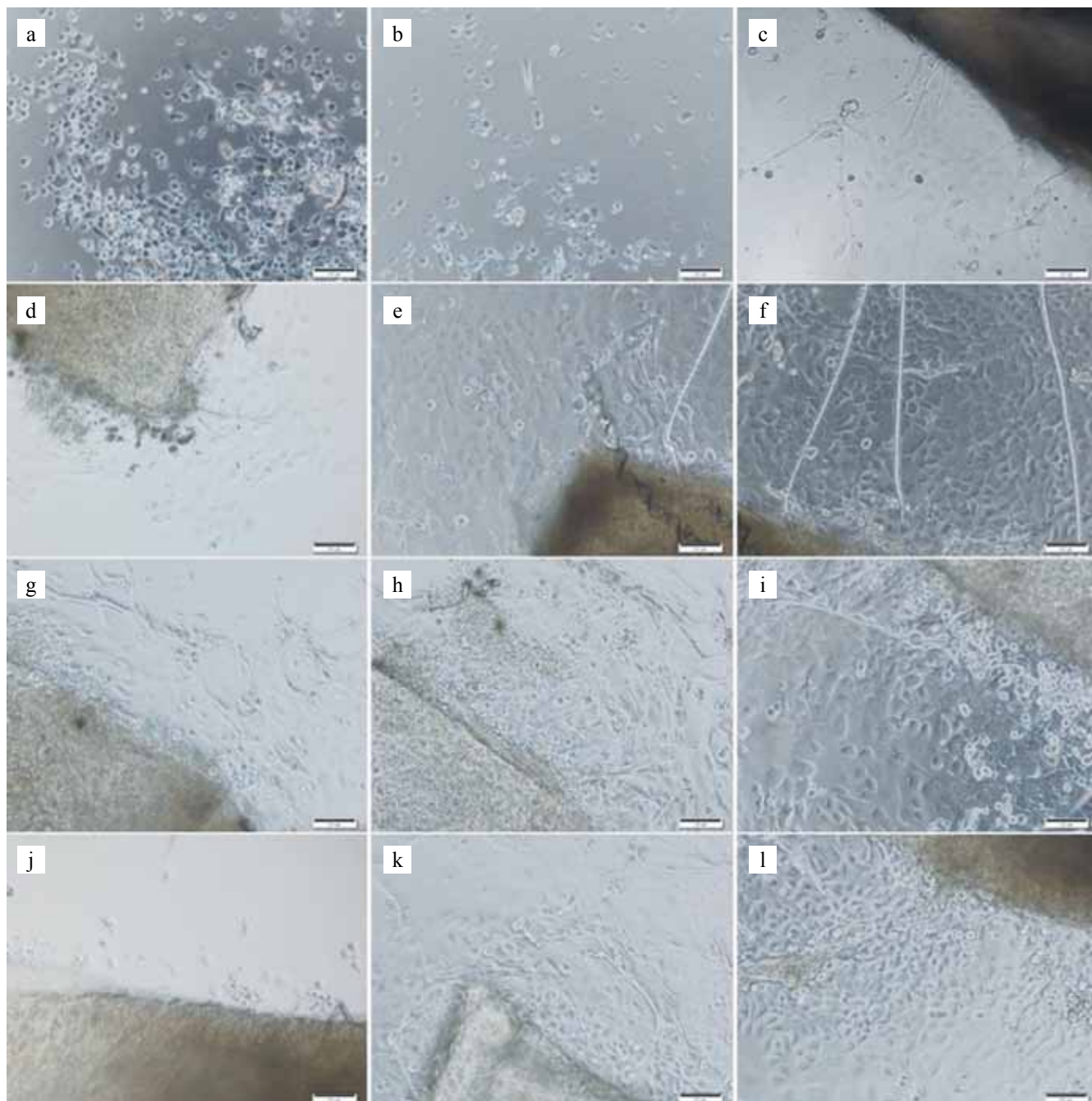


Fig. 4. Cell culture obtained from all types of mini-grafts on an EpiLife medium. Different observation times (horizontally from left to right – days 7, 11 and 14 of culturing, respectively). (a, b, c), cell culture from mini graft obtained using 100% FSL energy level; (d, e, f), cell culture from a mini graft obtained using 110% FSL energy level; (j, h, i), cell culture from a mini-graft obtained using 120% FSL energy level; (j, k, l), cell culture from a mini graft obtained using microsurgical instruments. Light phase-contrast microscopy. Magnification 100×

and “knife” methods of obtaining mini-grafts, where the best results came from the “laser” group ($p < 0.05$).

When determining the confidence limits using the modified Wald method, it was shown that on day 7, the confidence bounds in the “laser 100%” group were as follows [35%; 78%], “laser 110%” [57%; 98%], “laser 120%” [42%; 84%], “knife” [54%; 80%] (Fig. 5); and on day 14, the limits in the “laser 100%” group was [50%; 65%], “laser 110%” [80%; 92%], “laser 120%” [59%; 73%], “knife” [64%; 72%] (Fig. 6).

When calculating the confidence limits, the expected positive results on day 7 with 90% probability were obtained in the “laser 110%” and “knife” groups. On day 14, positive results were obtained in all groups. However, on day 14, maximum significant results were obtained in the “laser 110%” group (Diagram 2).

When calculating the probability of a positive event (we consider a positive event to be the attachment of a piece, as well as the attachment and active exit of cells from it) using the binomial test, it was revealed that in the “laser” group, with a one-sided sign test, the probability of getting a positive or successful result is 81.25% ($p = 0.003$). Accordingly, in the “knife” group, the probability of having a positive or successful result is 56.25% ($p = 0.029$).

Analysis of flow cytometry data

For immunophenotyping of the resulting cell culture along with analysis of the morphological picture, flow cytometry was performed. The cell cultures obtained on day 21 of cultivation of mechanically cut mini-grafts with FSL at 120% energy level were analyzed. We studied the expression levels of the following markers characterizing both MMSCs and LSCs: CD105 (endoglin) is a TGF- β III receptor available in endothelial cells, syncytiotrophoblasts, macrophages and connective tissue fibroblasts; in MMSCs, endoglin plays mainly a signaling role in the processes of chondrogenic differentiation and is involved in the interaction of MMSCs and hematopoietic cells in the bone marrow; CD90 (Thy-1, T cell differentiation antigen) is widely used for MMSCs phenotyping, expressed by proliferating cells; CD166 and CD29 are markers of cells starting their differentiation pathway and not yet belonging to a specific cell type; CD34 is a negative marker for MMSCs. As a result, according to flow cytometry data, a heterogeneous cell culture, containing an insignificant number of MMSCs and a prevalent number of LSCs, was obtained. The morphological picture of the two samples allowed us to conclude that phenotypically identical cell cultures were obtained in both cases (Table 4).

Cultivation of LSC of the 3rd passage on cell-free donor corneas

Examination of cell culture on the corneal surface using a phase-contrast microscope was extremely dif-

ficult because the corneal stroma tissue lost transparency under constant presence in the culture medium. After two weeks of observation, a histological examination of sections of the corneas under study was conducted. As a result, a monolayer of cells fixed to Bowman’s membrane was formed on all donor cornea samples. The cells were mostly small in size with a large polygonal nucleus, and spindle-shaped cells with a small nucleus were found among them. Groups of cells forming conglomerates were observed in the peripheral areas of the cornea during the formation of depressions (Fig. 7).

DISCUSSION

Currently, we are actively searching for an effective way to reconstruct the corneal epithelial layer in patients

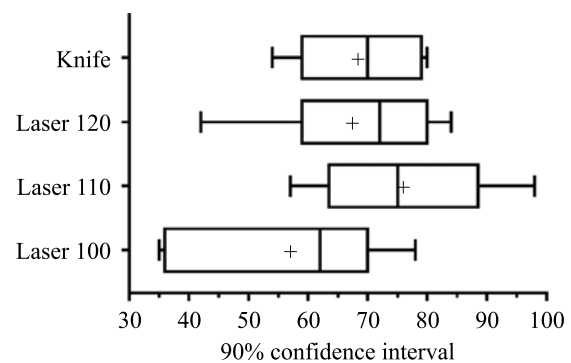


Fig. 5. Confidence limits on day 7 of observation in the test groups

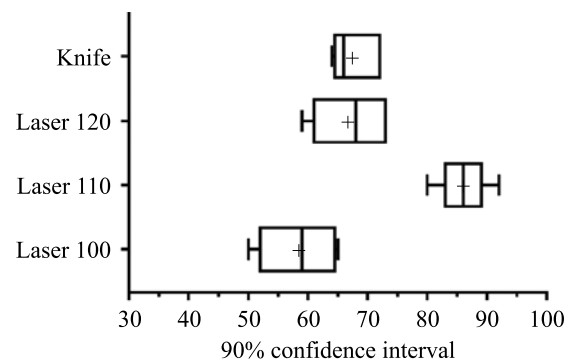


Fig. 6. Confidence limits on day 14 of observation in the test groups

Table 4

Immunophenotypic analysis of surface marker expression in a culture of passage 3 LSCs

Markers analyzed	Expression level	
	Femtosecond laser 120%	Knife
CD 105	0.49%	0.42%
CD 90	26.84%	28.26%
CD 166	99.89%	99.95%
CD 29	99.95%	99.96%
CD 34	0.11%	0.15%

with unilateral LSCD. Any surgical technique used for this disease should factor in the anatomical and functional features of the limbal zone.

The main component of the limbus is the limbal palisades of Vogt. These recesses have a unique gene expression and extracellular protein profile (extracellular matrix) that are specific and critical to LSC function. In the basal epithelial layer of the limbal niches, LSCs divide into identical cells in the horizontal plane or asymmetrically, thereby producing identical LSCs, and in the horizontal and vertical planes into transient amplifying cells (TACs). TACs then divide into postmitotic cells, which migrate centripetally. The postmitotic cells then differentiate into terminally differentiated cells (TDCs) and slough off the corneal surface. In addition to limbal epithelial progenitor cells, the limbal niche contains MMSCs, melanocytes, immune cells, vascular and neural cells, extracellular matrix and signaling molecules (growth factors and cytokines) [3–8].

MMSCs play a special role in LESC regulation. MMSC markers CD90 and CD105 are located beneath

the basal membrane of the limbal crypt and interact closely with LSCs [23–25]. MMSCs contact LSCs through several molecular substrates and signaling pathways that include aquaporin-1 and vimentin [26], chondroitin sulfate [24], SDF-1/CXCR4 [27], BMP/Wnt [28], and IL-6/STAT3 [29]. Additional mechanisms of interaction are through intercellular contacts, secretion of growth factors, and cytokine expression [30].

Evidence on the structure of the limbal niche and its microenvironment, which is necessary for its full functioning, indicate that it is essentially important to preserve all components of the limbal niche during surgeries that are aimed at restoring the corneal epithelial layer.

The current availability of FSLs in ophthalmic practice, capable of operating at the lowest energy levels, minimizing trauma and death of LSCs, makes the approach to the use of FSLs in corneal epithelium reconstruction more attractive.

It should be noted that the first results of femtosecond lasers application in keratolimbal allograft (KLAL) were described by Korean scientists in 2010. They performed

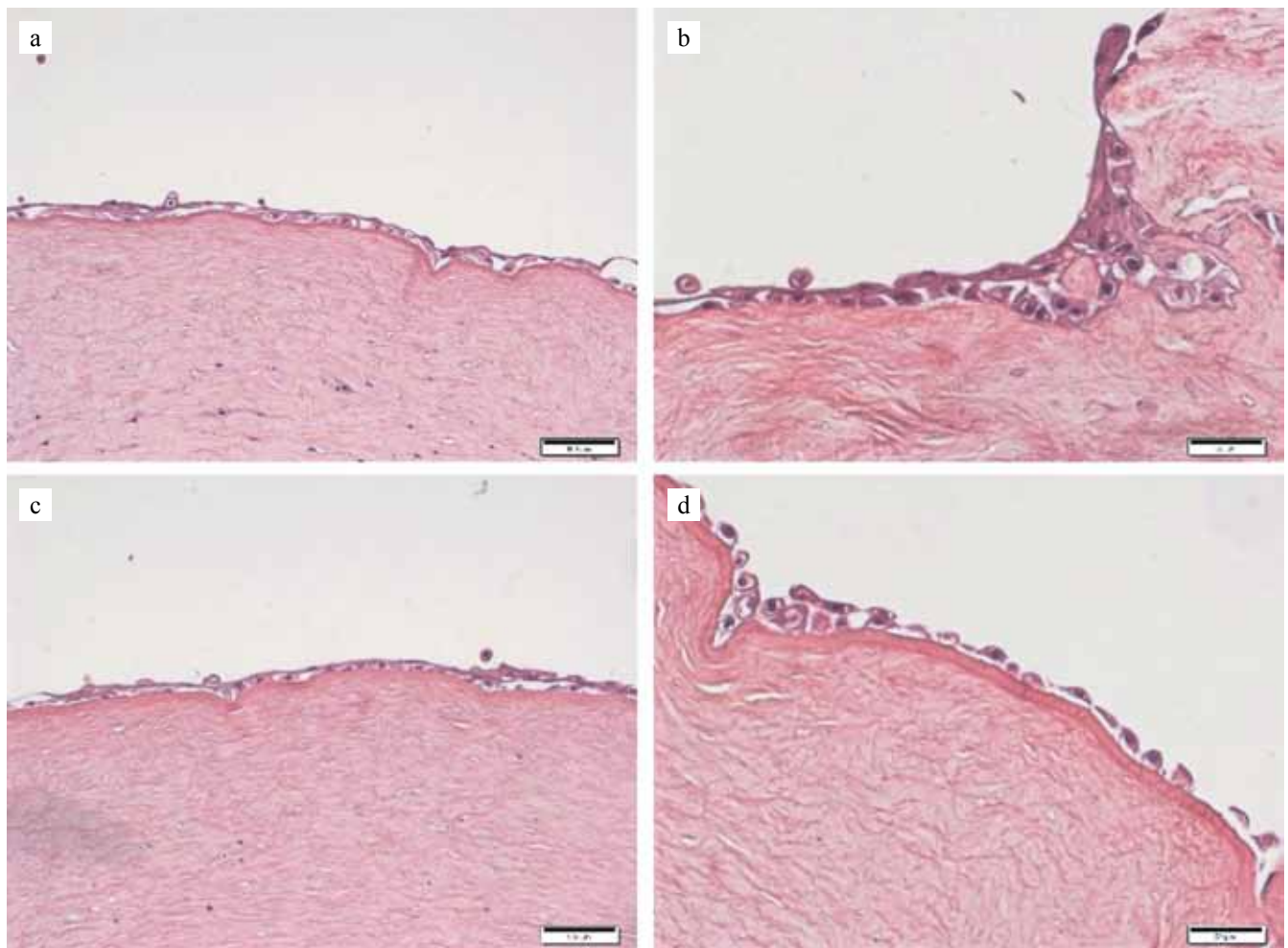


Fig. 7. Histological picture of donor inverted corneas with cell monolayer obtained from different cell cultures of the third passage. H&E stain: (a) culture obtained from a mechanically excised mini-graft, (c) culture obtained from a mini-graft excised by FSL at 100% energy, magnification 100×; (b) culture obtained from a mini-graft excised by FSL at 110% energy, (d) culture obtained from a mini-graft excised by FSL at 120% energy, magnification 50×

formation of a ring-type keratolimbal graft for further transplantation to the recipient. In this technology, a femtosecond laser (IntraLase, USA) was used to form a keratolimbal graft by cutting it out on the donor's eye so that only the distal border of the keratolimbal graft on the sclera side remained intact. It was cut out manually using a diamond knife because the appplanation ring used in the kit of this laser had a maximum diameter of 9.5 mm [31]. The authors noted that the use of FSL in KLAL technology allows to cut the graft predictably thin and significantly reduces the risks and time spent on graft formation.

Currently, the following laser systems are used in the Russian Federation: VisuMax (Carl Zeiss Meditec, Germany), IntraLase (Abbot medical optics, USA), LensX and WaveLight (Alcon, USA), Femto Visum (Optosystems, Russia) and Femto LDV Z8 (Ziemer, Switzerland). The latter two laser versions differ in that they operate at the lowest possible energy level, which is in the nanoJoule (nJ) range, which allows for tissue dissection with minimal wound healing reaction and apoptotic cells along the incision plane [32]. This effect is achieved by operating the laser at the lowest possible energy levels but with a higher cutting frequency [32]. This effect is achieved by operating the laser at the lowest possible energy levels, but with a higher cutting frequency. A distinctive feature of the Femto LDV Z8 laser (Ziemer, Switzerland) is the presence of a mobile handle that can be positioned on the eye at any necessary angle; this laser is also equipped with a built-in OCT system, which allows to make the laser operation predictable, controlled and safe.

In this work, we evaluated the safety and efficacy of the Femto LDV Z8 low-energy high-frequency FSL (Ziemer, Switzerland) in relation to LSCs. Its use in the clinic within the G-SLET technology will significantly reduce the operation time, minimize the risks of obtaining uneven and incomplete limbal graft.

In the EpiLife medium, there was a preferential yield of polygonal epithelial-like cells, while in the DMEM/F12 medium, a yield of MMSC-like cells was also observed. It is known that MMSCs are essential for full maturation of LSCs.

During the cultivation process, we were able to find out that the yield of cells from FSL-cut mini-grafts is higher (77.2%) than in the group with manual isolation of mini-grafts (63.6%). This indicates that the use of FSL allows for precise cutting of limbal mini-grafts at a programmed depth, capturing the entire limbal niche with all its surroundings.

When comparing the cell cultures obtained by cutting out (using FSL) mini-grafts at different energy levels, the highest cell yield was observed in the 120% laser energy level group. However, at the time of the first control examination, indicators in this group were lower than the others. This can probably be attributed to the

greater damaging effect of the energy on the peripheral borders of the mini-graft and the inhibition of the release of new cells overcoming the dead cell wall at the edges of the mini-graft. The higher number of cells (87.5%) in the obtained culture at the last observation period may indicate complete laser cutting out of all the necessary elements of the limbal niche functioning in a complex, without additional manipulations at the moment of evacuation of the mini-graft from the limbal bed, which was observed in the "laser 100%" and "laser 110%" groups. It should also be taken into account that statistical analysis showed that the probability of the mini-graft successfully adapting was higher in the "laser 110%" group.

CONCLUSION

This work presents a protocol for culturing limbal mini-grafts obtained using FSL, demonstrating active LSC growth. Cell cultures obtained from FSL-cut mini-grafts can grow for a long time, at least for 21 days. This indicates that FSL application in G-SLET technology is safe.

The use of FSL allows for precision cutting out of limbal mini-grafts at a controlled depth with its simultaneous fragmentation. This seems to us safer and more effective than the traditional mechanical "knife" cutting technique. This method has real prospects for further introduction into clinical practice.

The authors declare no conflict of interest.

REFERENCES

1. Thoft RA, Friend J. The X, Y, Z hypothesis of corneal epithelial maintenance. *Invest Ophthalmol Vis Sci.* 1983; 24: 1442–1443.
2. Del Monte DW, Kim T. Anatomy and physiology of the cornea. *J Cataract Refract Surg.* 2011; 37: 588–598.
3. Parfitt GJ, Kavianpour B, Wu KL, Xie Y, Brown DJ, Jester JV. Immunofluorescence tomography of mouse ocular surface epithelial stem cells and their niche microenvironment. *Invest Ophthalmol Vis Sci.* 2015; 56: 7338–7344.
4. Grieve K, Ghoubay D, Georgeon C, Thouvenin O, Bouheraoua N, Paques M et al. Three-dimensional structure of the mammalian limbal stem cell niche. *Exp Eye Res.* 2015; 140: 75–84.
5. Ramirez BE, Victoria DA, Murillo GM, Herreras JM, Calonge M. In vivo confocal microscopy assessment of the corneoscleral limbal stem cell niche before and after biopsy for cultivated limbal epithelial transplantation to restore corneal epithelium. *Histol Histopathol.* 2015; 30: 183–192.
6. Massie I, Dziasko M, Kureshi A, Levis HJ, Morgan L, Neale M et al. Advanced imaging and tissue engineering of the human limbal epithelial stem cell niche. *Methods Mol Biol.* 2015; 1235: 179–202.
7. Nubile M, Curcio C, Dua HS, Calienno R, Lanzini M, Iezzi M et al. Pathological changes of the anatomical

- structure and markers of the limbal stem cell niche due to inflammation. *Mol Vis.* 2013; 19: 516–525.
8. Notara M, Shortt AJ, O'Callaghan AR, Daniels JT. The impact of age on the physical and cellular properties of the human limbal stem cell niche. *Age.* 2013; 35: 289–300.
 9. Notara M, Refaian N, Braun G, Steven P, Bock F, Cursiefen C. Short-term uvb irradiation leads to putative limbal stem cell damage and niche cell-mediated upregulation of macrophage recruiting cytokines. *Stem Cell Res.* 2015; 15: 643–654.
 10. Kim BY, Riaz KM, Bakhtiari P, Chan CC, Welder JD, Holland EJ et al. Medically reversible limbal stem cell disease: clinical features and management strategies. *Ophthalmology.* 2014; 121: 2053–2058.
 11. Deng SX, Borderie V, Chan CC, Dana R, Figueiredo FC, Gomes JAP et al. Global Consensus on Definition, Classification, Diagnosis, and Staging of Limbal Stem Cell Deficiency. *Cornea.* 2019; 38 (3): 364–375.
 12. Malyugin BE, Gerasimov MYu, Borzenok SA, Golovin AV. Simple limbal epithelial transplantation (a literature review). *Fyodorov Journal of Ophthalmic Surgery.* 2019; (1): 77–86. [In Russ, English abstract]. <https://doi.org/10.25276/0235-4160-2019-1-77-86>.
 13. Sangwan VS, Basu S, MacNeil S, Balasubramanian D. Simple limbal epithelial transplantation (SLET): a novel surgical technique for the treatment of unilateral limbal stem cell deficiency. *Br J Ophthalmol.* 2012; 96: 931–934.
 14. Basu S, Sureka SP, Shanbhag SS, Kethiri AR, Singh V, Sangwan VS. Simple limbal epithelial transplantation: long-term clinical outcomes in 125 cases of unilateral chronic ocular surface burns. *Ophthalmology.* 2016; 123: 1000–1010.
 15. Malyugin BE, Gerasimov MY, Borzenok SA. Glueless simple limbal epithelial transplantation. The report of the first two cases. *Cornea.* 2020; 39 (12): 1588–1591. doi: 10.1097/ICO.0000000000002467.
 16. Borzenok SA, Gerasimov MYu, Komakh YuA, Khubetsova MKh, Tonaeva HD, Malikova LM, Plaksa PI. An algorithm for infectious screening of corneal donors in eye tissue bank of the S. Fyodorov Eye Microsurgery Federal State Institution. *Fyodorov Journal of Ophthalmic Surgery.* 2022; 2: 54–59. [In Russ, English abstract]. <https://doi.org/10.25276/0235-4160-2022-2-54-59>.
 17. Malyugin BE, Borzenok SA, Gerasimov MYu. Clinical outcomes of autologous cultured oral mucosal epithelium transplantation for treatment of limbal stem cell deficiency. *Fyodorov Journal of Ophthalmic Surgery.* 2020; 4: 77–85. [In Russ, English abstract]. <https://doi.org/10.25276/0235-4160-2020-4-77-85>.
 18. Borzenok SA, Malyugin BE, Gerasimov MYu, Ostrovsky DS. Cultivated autologous oral mucosal epithelial transplantation. *Russian Journal of Transplantation and Artificial Organs.* 2021; 23 (1): 171–177. [In Russ, English abstract] <https://doi.org/10.15825/1995-1191-2021-1-171-177>.
 19. Gerasimov MY, Ostrovskiy DS, Shatskikh AV, Borzenok SA, Malyugin BE. Labial mucosal epithelium grafting in an ex vivo human donor cornea model. *Exp Eye Res.* 2022; 216: 108931. doi: 10.1016/j.exer.2022.108931.
 20. Schindelin J, Arganda-Carreras I, Frise E, Kaynig V, Longair M, Pietzsch T et al. Fiji: an open-source platform for biological-image analysis. *Nat Methods.* 2012; 9 (7): 676–682. doi: 10.1038/nmeth.2019.
 21. Andjelic S, Lumi X, Vereb Z, Josifovska N, Facsko A, Hawlina M et al. A simple method for establishing adherent ex vivo explant cultures from human eye pathologies for use in subsequent calcium imaging and inflammatory studies. *J Immunol Res.* 2014; 2014: 232659. doi: 10.1155/2014/232659.
 22. Szabó DJ, Noer A, Nagymihály R, Josifovska N, Andjelic S, Veréb Z et al. Long-Term Cultures of Human Cornea Limbal Explants Form 3D Structures Ex Vivo – Implications for Tissue Engineering and Clinical Applications. *PLoS One.* 2015; 10 (11): e0143053. doi: 10.1371/journal.pone.0143053.
 23. Yamanda K, Young RD, Lewis PN, Shinomiya K, Meek KM, Kinoshita S et al. Mesenchymal-epithelial cell interactions and proteoglycan matrix composition in presumptive stem cell niche of the rabbit corneal limbus. *Mol Vis.* 2015; 21: 1328–1339.
 24. Dziasko MA, Armer HE, Levis HJ, Shortt AJ, Tuft S, Daniels JT. Localisation of epithelial cells capable of holo-clone formation *in vitro* and direct interaction with stromal cells in the native human limbal crypt. *PLoS One.* 2014; 9: e94283.
 25. Mathews S, Chidambaram JD, Lanjewar S, Mascarenhas J, Pranja NV, Muthukkaruppan V et al. In vivo confocal microscope analysis of normal human anterior limbal stroma. *Cornea.* 2015; 34: 464–470.
 26. Higa K, Kato N, Yoshida S, Ogawa Y, Shimazaki J, Tsubota K et al. Aquaporin 1-positive stromal niche-like cells directly interact with N-cadherin-positive clusters in the basal limbal epithelium. *Stem Cell Res.* 2013; 10: 147–155.
 27. Xie HT, Chen SY, Li GG, Tseng SC. Limbal epithelial stem/progenitor cells attract stromal niche cells by SDF-1/CXCR4 signaling to prevent differentiation. *Stem Cell.* 2011; 29: 1874–1885.
 28. Han B, Chen SY, Zhu YT, Tseng SC. Integration of BMP/Wnt signaling to control clonal growth of limbal epithelial progenitor cells by niche cells. *Stem Cell Res.* 2014; 12: 562–573.
 29. Notara M, Shroff AJ, Galatowicz G, Calder V, Daniels JT. IL6 and the human limbal stem cell niche: a mediator of epithelial-stromal interaction. *Stem Cell Res.* 2010; 5: 188–200.
 30. Poliseti N, Agarwal P, Khan I, Kondaiah P, Sangwan VS, Vemuganti GK. Gene expression profile of epithelial cells and mesenchymal cells derived from limbal explant culture. *Mol Vis.* 2010; 16: 1227–1240.
 31. Choi S, Kim J, Lee D. A New Surgical Technique: A Femtosecond Laser-Assisted Keratolimbal Allograft Procedure. *Cornea.* 2010; 29: 924–929.
 32. Riau AK, Liu YC, Lwin NC, Ang HP, Tan NY, Yam GH et al. Comparative study of nJ- and μJ-energy level femtosecond lasers: evaluation of flap adhesion strength, stromal bed quality, and tissue responses. *Invest Ophthalmol Vis Sci.* 2014; 55: 3186–3194. doi: 10.1167/iovs.14-14434.

The article was submitted to the journal on 07.05.2023